

OPEN ACCESS

The Protection Zone: A Long-Range Corrosion Protection Mechanism around Conducting Polymer Particles in Composite Coatings: Part II. PEDOT: PSS

To cite this article: A. Merz and M. Rohwerder 2019 *J. Electrochem. Soc.* **166** C314

View the [article online](#) for updates and enhancements.



PRIMETM
PACIFIC RIM MEETING
ON ELECTROCHEMICAL
AND SOLID STATE SCIENCE
2020

Abstract Submission
DEADLINE EXTENDED:
May 29, 2020

Honolulu, HI | October 4-9, 2020







The Protection Zone: A Long-Range Corrosion Protection Mechanism around Conducting Polymer Particles in Composite Coatings: Part II. PEDOT: PSS

A. Merz and M. Rohwerder *,^z

Max-Planck-Institut für Eisenforschung GmbH, 40237 Düsseldorf, Germany

PEDOT:PSS is most likely the intrinsically conducting polymer (ICP) with the most outstanding stability of its electrical properties. Thus it might be the ideal material when high-performance coatings for corrosion protection of metal products are of aim. The purpose of this work is to elucidate the protection against corrosion provided by PEDOT:PSS pigments when used as an additive in a conventional insulating coating, applied to iron and zinc. By means of dedicated model samples simulating ICP pigments in contact with the metal surface on a more macroscopic level, it was found that a “protection zone” is established in the vicinity of the ICP, hindering further coating delamination. Resistance against ionic transport at the coating/metal interface is of major significance for its endurance, as the functioning of the protection zone relies on galvanic polarization of the interface by the ICP. Scanning Kelvin Probe (SKP) has been employed to monitor the changes in corrosion potential, in order to evaluate and also compare the PEDOT:PSS performance to other ICPs available in the market, e.g. polyaniline and polypyrrole.

© The Author(s) 2019. Published by ECS. This is an open access article distributed under the terms of the Creative Commons Attribution Non-Commercial No Derivatives 4.0 License (CC BY-NC-ND, <http://creativecommons.org/licenses/by-nc-nd/4.0/>), which permits non-commercial reuse, distribution, and reproduction in any medium, provided the original work is not changed in any way and is properly cited. For permission for commercial reuse, please email: oa@electrochem.org. [DOI: 10.1149/2.0981912jes]



Manuscript submitted May 15, 2019; revised manuscript received July 12, 2019. Published July 19, 2019. This was Paper 776 presented at the National Harbor, Maryland Meeting of the Society, October 1–5, 2017.

Poly(3,4-Ethylenedioxythiophene)-Poly(Styrene Sulfonate) (PEDOT:PSS) is an excellent material regarding its high thermal and electrochemical stability in the doped form.¹ It is nowadays employed as a transparent and thin conductor for electronic and optical gadgets, such as in Organic Light Emitting Diodes (OLEDs),² stretchable displays, organic solar cells, supercapacitors and fuel cells.³ Furthermore, PEDOT:PSS shows high electrical conductivity and good film-forming ability,⁴ properties which make it a promising candidate to be applied in coatings for corrosion protection.

Organic coatings are extensively used to protect metallic substrates from corrosion. Currently, for reliable performance, coatings often contain inorganic pigments such as metal oxides, salts or metallic pigments.⁵ These pigments usually are able to leach corrosion inhibitors in humid conditions. However, as most inhibitors have certain chemical activity and often contain heavy metal, there is always the risk of detrimental effects on human health and the environment, which is undesirable.

The Intrinsically Conducting Polymers (ICP's), which were discovered at the end of the 20th century by Heeger, MacDiarmid and Shirakawa,^{6–8} constitute a promising alternative approach to provide high delamination resistance to organic coatings. Up to now, the real efficacy of the ICPs and the mechanisms which take place in corrosion protection are still controversially discussed and questioned,^{9–11} however it was shown that when certain design aspects are obeyed the resistance against corrosion-driven coating delamination can be enhanced.^{9,12} Merz et al.¹² showed that polyaniline and polypyrrole, when applied as disconnected particles (such as additives in a composite coating) on iron or zinc, are able to inhibit the oxygen reduction at the delamination front when it comes close enough to the ICP, forming a “protection zone” where no or very slow coating delamination occurs. This protection zone is formed as a result of galvanic polarization of the interface between the metal surface and the coating by the ICP. This prevents the decrease of the potential at the delamination front and thus inhibits the onset of oxygen reduction and hence of delamination, as was shown in our prior work.¹² In that work, the formation of the protection zone around the ICP was demonstrated for polypyrrole and for polyaniline as ICP.

In this work, we show by a comprehensive and comparative study how protective such a protection zone around PEDOT:PSS is. For that,

dedicated model samples of PEDOT:PSS islands (dots) applied onto iron and zinc samples and coated by an insulating coating of Polyvinyl Butyral (PVB) were prepared. The corrosion protection efficiency and the protection mechanisms were analyzed mainly through the application of the Scanning Kelvin Probe technique for in-situ monitoring the delamination progress, and elemental analysis of the interface by X-ray Photoelectron Spectroscopy (XPS) after pulling off the delaminated and partially delaminated PVB coating.

Experimental

Materials.—Iron and zinc plates (99.999%) with a thickness of 1.5 mm were purchased from Goodfellow and prepared as in Part I.¹²

Poly(3,4-Ethylenedioxythiophene)-Poly(Styrene Sulfonate) with a concentration of 0.8% in water was purchased from Sigma-Aldrich and used as received. The reagent was kept in a refrigerator until use. Potassium chloride (KCl) and PVB (MW = 50.000–80.000 g/mol) were also obtained from Sigma-Aldrich and used as received. All aqueous solutions were prepared using purified water from a USF ELGA system, which provides water with a conductivity of less than 0.055 $\mu\text{S}/\text{cm}$.

Deposition of PEDOT:PSS.—The highly conductive chemical acquired was directly applied to the metallic substrates through a simple drop-casting method. For the studies reported here the PEDOT was applied as small dots onto the metal surface, thus simulating ICP pigments in a composite coating applied onto the metal, similar to our previous work.¹² The coating preparation consisted of the following steps:

1. Using a microliter pipette selected to prepare dots of 2 mm diameter (the diameter of the dot relies on the chosen pipette) 0.5 μl of PEDOT:PSS was drop-casted onto iron or a zinc surface.
2. Secondly, the samples were dried for 15 minutes at 75°C.
3. Then a coating of polyvinyl butyral (PVB) was applied, which serves to simulate the non-conductive matrix of composite coating containing pigments of ICP. This preparation step is further detailed below in section Preparation of the model samples.

Preparation of the model samples.—The PVB coating was prepared from 10 wt% PVB dissolved in ethanol that was spin-coated twice at 2000 rpm during 20 s onto the sample. This results in a coating thickness of about 2 to 3 micrometers.¹³ PVB was selected as

*Electrochemical Society Member.

^zE-mail: m.rohwerder@mpie.de

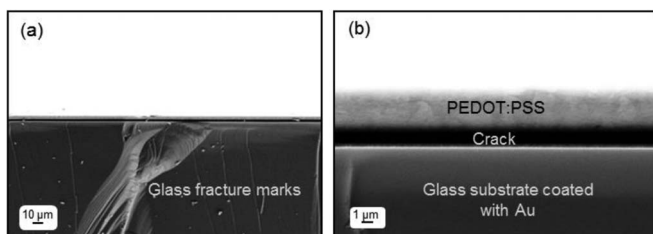


Figure 1. Cross section images of a 0.5 μl PEDOT:PSS film deposited on a gold substrate, acquired via SEM. In (a) it can be seen that the PEDOT:PSS possesses a homogenous thickness over the whole sample. In (b) a close-up image shows that the PEDOT:PSS is circa 3 μm thick.

coating as it shows relatively fast delamination behavior, allowing to perform a delamination experiment in a few days.

Application of PVB onto the locally PEDOT:PSS coated sample led to the formation of a PVB/PEDOT:PSS model composite coating. Lastly, by using an epoxide paste the sample is bonded to another metal plate. By using epoxy resin for building up borders, an artificial defect was prepared (see also part I),¹² which is filled with electrolyte (aqueous 1 M KCl).

Thickness measurements.—In order to get information about the thickness of the PEDOT:PSS dots, a single dot was drop-casted onto an ultra-smooth gold film evaporated on glass. The sample was then broken by hand and its cross-section was analyzed with the use of a Scanning Electron Microscope (SEM LEO 1550 VEP).

Methods used for investigating the corrosion protection.—In order to investigate how the delamination front progresses and the efficacy of the “protection zone”, the prepared PEDOT:PSS/metal samples were introduced in a humidified (relative humidity = 95%) Kelvin probe chamber. A commercial SKP system from KM Soft Control was utilized with a 100 μm thick Ni(80)/Cr(20) tip. Before starting any measurement the SKP tip was calibrated vs. a Cu/sat. CuSO_4 reference and all potentials in the following are referred to the Standard Hydrogen Electrode (SHE).¹⁴ During the measurement, the SKP tip scans an area that ranges from close to the defect up to 6500 μm away from it. The data attained shows the potential distribution as a function of time and distance from the defect.

In this way also the gradual failure of the protection zone, which is associated with the ongoing reduction of the PEDOT:PSS dot was investigated. Any ICP reduction has to be accompanied by the ionic migration along with the PVB/metal interface, in order to close the electrical circuit. The two possible ways for this to happen are: (1) the ICP is incorporating cations, which are being delivered from the electrolyte (KCl) in the defect, or (2) the counter-anions, which initially provide charge neutrality to the ICP, are now expelled from the polymer. To identify which of these mechanisms is occurring during the polymer reduction, X-ray Photoelectron Spectroscopy (XPS) investigation of the interface after pulling off the coating was utilized, as it is capable of identifying and quantifying the ions present at the sample's surface.

Results and Discussion

PEDOT:PSS thickness result.—Prior to the delamination experiments it was tried to obtain information about the thickness of the applied PEDOT:PSS dots. This was done by applying PEDOT:PSS on a gold coated glass sample, which was then broken and the cross section analyzed with SEM (see Fig. 1). As can be seen the thickness of the PEDOT:PSS was about 3 μm . A typical result of the effect of PEDOT:PSS dots on delamination of PVB on iron is shown in Fig. 2, obtained with a double-dot arrangement.

Effect of PEDOT:PSS on the delamination behavior of PVB on iron.—Fig. 2a schematically shows the typical position and length

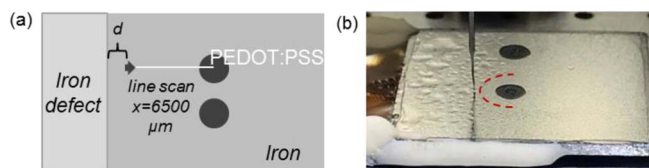


Figure 2. (a) Schema of the double-dot arrangement of a PEDOT:PSS/Fe sample, indicating the direction and position of the line scan (scan length $x = 6500 \mu\text{m}$ and distance from the edge $d = 2000 \mu\text{m}$) – the measured potential profiles are shown in Fig. 3. (b) Photo of the sample during experiment (after 100 hours), showing the double-dots and the protection zone, which is clearly visible due to an electrolyte droplet accumulation that occurs in the delaminated area after longer times (see indication of the protection zone by dashed red line).

of the line scan measured with SKP, here for a double-dot arrangement. And Fig. 2b shows a photo of the sample during the experiment after 100h of measurement. After such long time the delaminated area becomes directly visible due to PVB coating lift off by accumulation of electrolyte which appears in form of droplet/blister like features. As can be seen there is a zone around the PEDOT:PSS dots where no such features are visible. This is the protection zone.

The evolution with time for potential profiles obtained from the SKP measurement is shown in Figs. 3a–3c, while Fig. 3d depicts the sample at the end of the delamination experiment. The interval between two consecutive curves is circa 20 minutes. The first scan shows the potential profile before the onset of the delamination (horizontal bold black curve in Fig. 3a), while the black vertical line represents the edge of the PEDOT:PSS dot. Surprisingly, the start potential measured on the PEDOT:PSS dot is very low even though the dot is undamaged at this point. This can only mean that the PEDOT:PSS/Fe system is in a so-called Fermi misalignment state, i.e. an insulating layer has been formed between the PEDOT:PSS and the Fe substrate,^{15,16} accompanied by interfacial charging between PEDOT and Fe, leading to an apparently lower potential.¹⁷ Fundamental insight into Fermi level misalignment was gained in prior work especially with PANi and PPy applied on Fe and Zn.^{16,17} These in-depth SKP studies of PANi and PPy have shown that the corrosion induced by the galvanic coupling between PANi and particularly zinc can result in the formation of an insulating interfacial layer, e.g. through the dedoping of PANi emeraldine salt to emeraldine base (EB) upon contact to amphoteric zinc(hydr)oxide as proposed by Williams and McMurray.¹⁸ The layer prevents the electron transport from the metal to the conducting polymer, which results in an electronic de-coupling of the ICP from the metal and a negative charging on the metal side and a positive one on the ICP side, which causes the (apparent) potential measured over the PANi to be found even lower than the potential of the PVB coated metal.

However, in order to provide corrosion protection based on the protection zone effect, or based on the triggered release of stored active agents by ICP reduction, the ICP must show a proper electronic coupling to the metal as it needs to be galvanically coupled to the PVB/metal interface surrounding areas of ICP/metal. Vimalanandan et al.,¹⁵ showed that electronic coupling can be achieved for such cases by preventing direct contact between the ICP and the metal, e.g. by decorating the PANi particles with conducting spacer-particles (such as gold nanoparticles). By doing that the PANi does not make direct contact to the zinc surface. The electronic contact between zinc and PANi is then established over the spacer particles.

In the case of PEDOT:PSS applied in this work, no special procedure was needed to circumvent the formation of the insulating layer between ICP and metal, since the edge of the dot showed, from the beginning, a quite high potential, indicating that there no Fermi level misalignment seems to be present, i.e. electronic coupling between ICP and metal should be present. That would mean that this region, of higher potential at the outer fringes of the ICP dot, is not electronically coupled to the ICP in the middle of the dot, where the low potentials

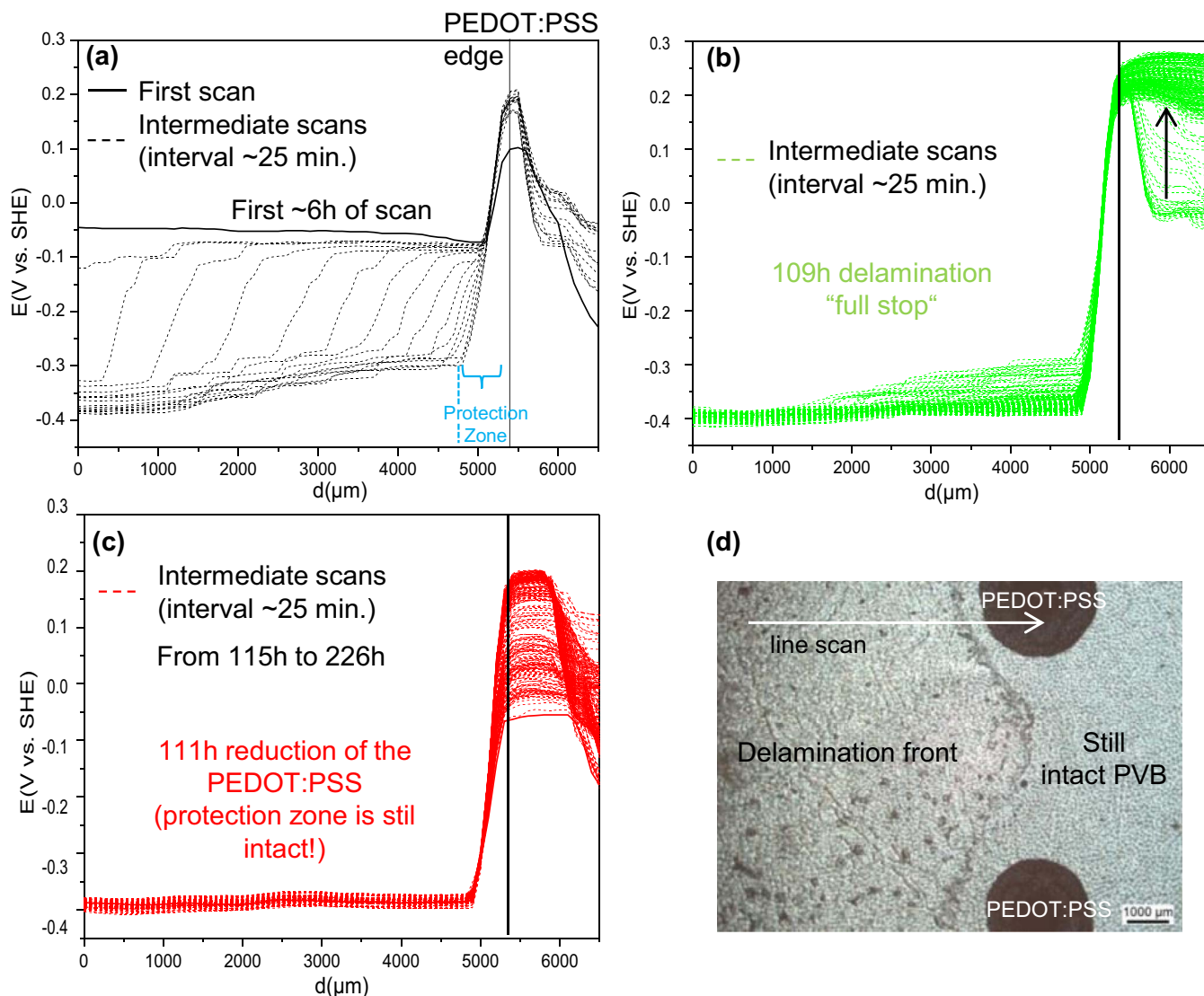


Figure 3. Delamination progress measured with SKP on a PEDOT:PSS/Fe sample, with PVB as topcoat. The black vertical line designates the border of the dot. In (a) the delamination at the interface PVB/Fe and the low potential of the PEDOT:PSS, due to the Fermi level misalignment, can be seen. In (b) the 109 h “full” stop at the protection Zone as well as the realignment of the Fermi level (indicated by the arrow) is shown. In (c) the slow reduction of the PEDOT:PSS can be seen, from 115 h after the experiment was started to its end after 226 hours. And in (d) the microscopic optical image of the sample after the termination of the experiment evidencing still intact protection zones even after 226 hours. The delamination did not advance through the space between the dots; in fact the effect of the protection zone extends quite far.

are measured. It is assumed here that this is similar as discussed by Rohwerder et al.¹⁶ for ICP films applied over Fe/Zn couples: while for PPy/Zn Fermi level misalignment was observed, this was not the case for PPy/Fe. At the borderline between the two, steady corrosion led to the bulk reduction of the PPy at this borderline, until the two regions were separated electronically.

The absence of Fermi level misalignment at the border of the PEDOT:PSS dots might be due to a faster drying there, which means a shorter reaction time until drying. Most likely at the border, the time is too short for forming an fully insulating interfacial layer.

Interestingly here is that, once the delamination front comes close to the PEDOT:PSS, a slow Fermi level re-alignment process seems to be initiated, as can be seen from the slowly increasing potentials measured on the PEDOT (see Figs. 3a–3b). This was also observed for the case when a PEDOT coating on top of zinc, which also showed Fermi level misalignment, was in direct contact with electrolyte in an artificial defect.¹⁵ It is assumed that the contact with the electrolyte enables, by enhancing lateral ion mobility, slow annihilation of the charge separation across the insulating layer at the interface that is the

cause for the misalignment.¹⁷ Also, the electronic coupling between the PEDOT:PSS and the metal seems to be reestablished, most likely because the electrolyte has a modifying effect on the insulating interfacial layer. Due to the re-establishment of the electronic coupling for the PEDOT:PSS employed in this work, the PEDOT:PSS was able to build up a protection zone, providing an extremely high level of delamination inhibition. Indeed, it seems that the re-establishment of the electronic coupling and formation of the protection zone is going hand in hand.

As already discussed, in Fig. 3b the potential measured over the dot increases from curve to curve until it reaches the normal potential value for PEDOT:PSS (circa 300 mV, i.e. full Fermi level alignment), and a protection zone is formed. Fig. 3b also shows that the delamination front is stopped at the protection zone for circa 109 hours without observable reduction of the PEDOT (although some has to occur to provide the polarization as that is what makes the protection zone). After that, the PEDOT:PSS slowly started to be visibly reduced, but the delamination front still halted (Fig. 3c). The experiment was terminated after ~226 hours, still displaying an intact protection zone

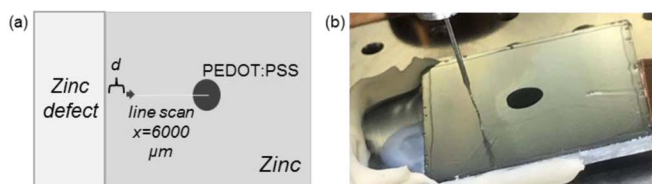


Figure 4. (a) Schematic drawing of the single dot arrangement of the PEDOT:PSS/ zinc sample, indicating the direction and position of the line scan (scan length $x = 6000 \mu\text{m}$ and distance from the edge $d = 2000 \mu\text{m}$). (b) PEDOT:PSS sample during the measurement at the SKP, showing the formation of the protection zone.

as well as no progress of the delamination in between the dots (see Fig. 3d).

Effect of PEDOT:PSS on the delamination behavior of PVB on zinc.—Also for PEDOT:PSS applied onto zinc, similar experiments were carried out. Fig. 4a shows the set up for a sample with a single

dot of PEDOT:PSS applied to zinc and coated by PVB, and Fig. 4b is a photo made during the experiment.

The line scan performed advanced from left to right, i.e. from close to the defect up to the middle of the dot, with a total extent of “ x ” = 6000 μm and the PEDOT:PSS border being at “ x ” $\sim 5400 \mu\text{m}$. In Fig. 5 the potential profiles are consecutively shown. As seen from the first profile in Fig. 5a, also in the case of PEDOT:PSS/ Zn Fermi level misalignment is present at first. The time between each curve shown in Fig. 5 is circa 11 min., i.e. the delamination front advanced quickly until the protection zone was reached. Again the Fermi level misalignment is slowly lifted and a protection zone forms. The delamination is nearly fully stopped in front of the protection zone (see also Fig. 4b) for circa 10 hours (see Fig. 5b). Next, a now visible slow reduction of the PEDOT:PSS starts to take place (red curves at Fig. 5c).

The last curve was measured after ~ 20 hours and it shows in the delaminated area potentials that are significantly higher (circa 0.1V) than in the delamination curves at the beginning. This is assumed to be caused by the accumulation of corrosion products that are forming at the interface over such long duration of the experiment. Different from the delaminated coating/iron interface, at the delaminated

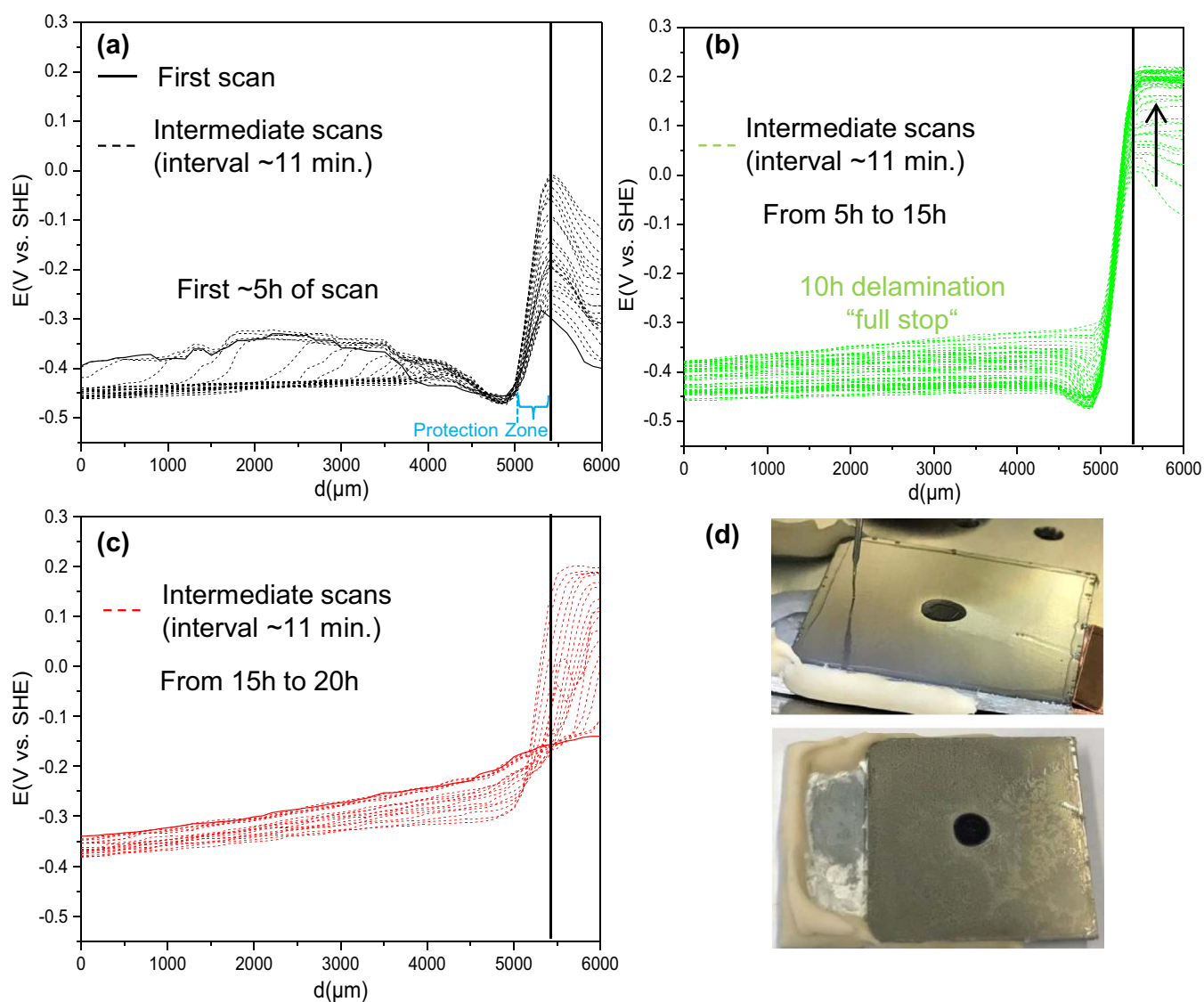


Figure 5. Delamination progress on a zinc sample with a $\sim 2 \text{ mm}$ diameter PEDOT:PSS dot and PVB as topcoat. In (a) potential profiles obtained in the first 5 h of delamination of the interface PVB/ zinc are shown and the Fermi level misalignment can be clearly seen, which already starts to be lifted; in (b) a 10 hours nearly full stop at the protection zone as well as the further realignment of the Fermi level is observed; in (c) the following slow visible reduction of the PEDOT:PSS can be seen; and in (d) an image of the sample after circa 20 hours of experiment is depicted, evidencing the complete delamination of the PVB coating, while the PEDOT:PSS dot and a small zone surrounding are still intact.

coating/zinc interface zinc corrosion occurs at the elevated pH levels caused by the oxygen reduction at the interface (while the Fe stays passive under these conditions). This corrosion product accumulation seems to increase the resistance for ion transport along the delaminated interface, which results in an increase in the potentials far away from the defect. This should also lower the driving force for delamination. However, overall on zinc, a much thinner and circa 10 times less effective protection zone is observed. One fact causing this reduced protection might be the zinc corrosion at the delaminated area. It is likely that this also slowly proceeds into the protection zone, making it slowly thinner. Another aspect might be the higher ion mobility at the PVB/metal(oxide) interface compared to iron. As will be shown below, only cation mobility at the interface is here of importance for the interfacial polarization. And this appears to be much faster for the PVB/zinc than for the PVB/iron interface. However, quantification is not easy and is the subject of current research.

To summarize, the results obtained for the performance of the protection zone around isolated PEDOT:PSS dots applied onto Fe or Zn, simulating the behavior of pigments in composite coatings, indicate that the performance of the PEDOT:PSS, when compared to other ICPs submitted to similar experimental conditions, is superior (see part I).¹² Since no inhibiting ions are released here and the PVB/metal interface is not affected by the type of ICP used for the ICP dot, it is proposed that PEDOT:PSS is able to polarize the PVB/metal interface even at very low reduction currents, leading to its very slow reduction and thus to the very long duration of the protection. This means that the interfacial resistance “*R*” for the ion current along the interface of the protection zone has to be very high for this ICP. However, as already mentioned, the PVB/metal interface must be independent of the ICP, thus the only possible explanation would be that the dominating type of migrating ion in the protection zone might be different for the ICP. In recent work, it was convincingly shown that cations and anions can have significantly different mobility along coating/metal interfaces and that this can affect the delamination kinetics.¹⁹ The only way the ICP can influence the dominating type of migrating ions is by its preferred way of charge neutralization during electrochemical reduction. For PANi and PPy we have already shown that the ions providing the polarization in the protection zone around isolated islands of these are the counter-anions being expelled from the ICP during reduction.¹² Hence, it seems logical that this has to be different for PEDOT:PSS. In order to find out whether this is the case, the elemen-

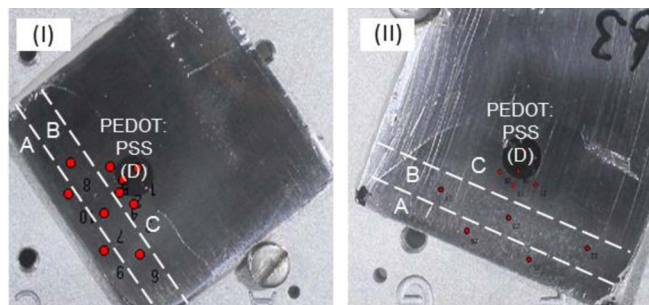


Figure 6. PEDOT:PSS/Fe samples. Samples I and II were delaminated for 6 and 8 hours respectively before their PVB coating was manually removed. The sample is divided in 4 zones: A-D, in which the red points indicate the exact location of measurement.

tal composition of the interface was investigated by XPS. The results are shown in the next section XPS results for PEDOT:PSS samples.

XPS results for PEDOT:PSS samples.—Delaminated model samples with PEDOT:PSS dots were all equally prepared so that a direct comparison between them is possible. The distance between the edge of the sample and the conducting polymer dot was maintained equivalent to ~ 7 mm and the delamination time was established to 6 or 8 hours, in order to analyze the period just after the protection zone has formed. Separate XPS measurements for all peaks of C1s, O1s, N1s, S2p, Cl2p, K2p, and Fe2p3 were acquired with 0.1 eV resolution (Quantum 2000 Microprobe ESCA, PHI). Examples of evaluated points are shown in Fig. 6.

Through this measurement, it was determined whether the PSS anion is being expelled from the PEDOT matrix or if potassium cations, migrating from the defect, are being incorporated into the polymer matrix. Table I shows the average atomic concentrations for samples I and II in the regions A to D (regions are indicated in Fig. 6), where A and B represent the delaminated area, C the protection zone and D the surface of the PEDOT:PSS. 0.6 or 0.8% of K in the PEDOT may seem quite small compared to the much higher values found in the delaminated interface and the protection zone. However, while there

Table I. Average atomic concentration at regions A-D of the PEDOT:PSS samples, sulfur and potassium are highlighted since they are the most important elements in this investigation.

Average atomic concentration (%) of:		Measured regions:			
		A ¹	B ²	C ³	D ⁴
SAMPLE I (6h)	S2p	0.00	0.00	0	5.40 ± 0.48
	K2p	15.15 ± 0.36	9.90 ± 0.7	6.35 ± 0.15	0.62 ± 0.2
	C1s	14.57 ± 0.78	25.89 ± 0.17	25.50 ± 1.1	58.68 ± 2.3
	N1s	1.78 ± 0.1	2.38 ± 0.28	5.40 ± 1.1	8.83 ± 0.26
	O1s	57.25 ± 2.6	50.96 ± 0.71	49.55 ± 1.57	26.12 ± 1.1
	Cl2p	1.13 ± 0.16	0.42 ± 0.08	0.00	0.00
SAMPLE II (8h)	Fe2p3	10.12 ± 0.11	10.45 ± 0.19	13.20 ± 0.5	0.35 ± 0.2
	S2p	0.00	0.00	0.00	6.03 ± 0.16
	K2p	21.99 ± 1.0	16.62 ± 0.5	4.70 ± 0.07	0.82 ± 0.18
	C1s	12.65 ± 1.2	20.32 ± 0.5	26.35 ± 1.96	62.48 ± 0.76
	N1s	0.00	0	1.62 ± 0.1	8.30 ± 0.15
	O1s	56.40 ± 1.63	54.09 ± 0.86	52.67 ± 1.12	21.97 ± 0.71
Cl2p	0.65 ± 0.07	0.66 ± 0.02	0.00	0.00	
Fe2p3	8.31 ± 0.7	8.31 ± 0.89	14.66 ± 0.81	0.4 ± 0.2	

A¹: region closest to the artificial defect.

B²: region in between the defect and the protection zone.

C³: protection zone.

D⁴: over the ICP.

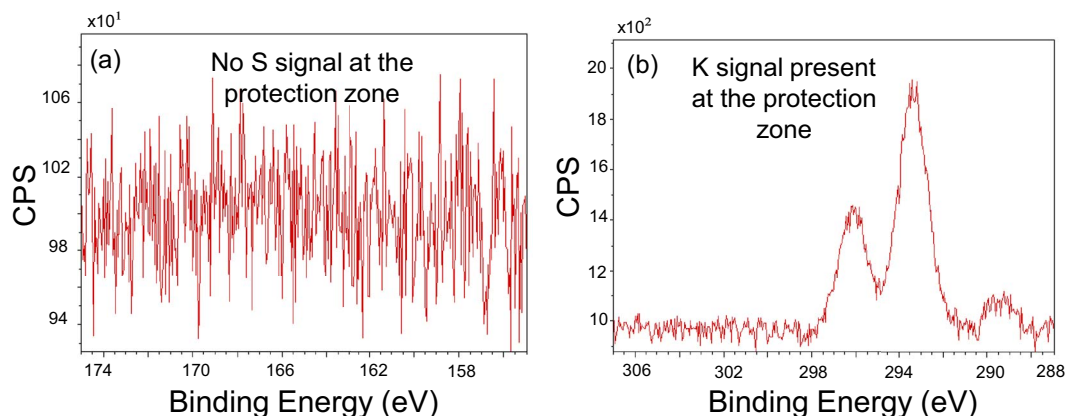


Figure 7. XPS spectra of sulfur (a) and potassium (b) in the protection zone of the PEDOT:PSS sample (II). From (a) can be deduced that S anion is not present outside the PEDOT:PSS, while (b) shows that K cations are present.

the K is just in the nanoscopic volume at the interface, in the PEDOT it is incorporated into a dot of more than a micrometer thickness.

From Table I and from the detailed spectra of K2p and S2p obtained in the protection zone (see Fig. 7), it can be seen that no S was found in regions A, B or C, however significant amount of K2p was detected in these regions.

This means that the large aromatic PSS anion is immobile and is trapped inside the PEDOT matrix, while the K^+ migrates from the defect in direction of the polymer dot, crosses the protection zone and is incorporated into the PEDOT:PSS, as shown in the spectra of Fig. 8.

So, the XPS results clearly showed that the PEDOT:PSS possesses a behavior in its charge neutralization during reduction which differs from other ICPs, such as polyaniline and polypyrrole. The latter, when applied as isolated islands at the interface, releases their counter-anions during reduction,¹² while the PEDOT:PSS incorporates cations instead. This difference is essentially due to the aromatic counter-anion, the polystyrene sulfonate (PSS), which cannot be expelled from the ICP matrix, i.e. the ICP has to take up the cations migrating from the defect for charge neutralization. It was observed that this uptake occurs at a low rate, which is attributed to a higher resistance for cation mobility at the investigated PVB/metal interface than for anion mobility, which results in a similar " $i \cdot R$ " potential drop across the protection zone at a much smaller current " i ". Hence the PEDOT:PSS reduction is very slow, and thus pronounced long-term corrosion protection can be provided.

For this it is important that discrete particle of ICP are in contact with the metal at the interface. In addition, it was shown that a configuration of discrete islands of ICPs is capable of increasing the

resistivity of the whole pattern against delamination, especially when their protection zones overlap.

Conclusions

In this work the protection zone mechanism for corrosion protection as it might be provided by PEDOT:PSS containing composite coatings was investigated by using dedicated model samples, on iron and zinc. It was shown that in the surrounding area of a PEDOT:PSS dot, a pull-down of the potential at the delamination front is prevented. This prevention of potential decrease also inhibits the onset of oxygen reduction at the interface, which in turn hinders or at least slows down any further coating delamination. The effect is more significant for PEDOT:PSS than for other ICPs such as PPy and PANI, which is proposed to be due to the fact that here the polarization at the interface in the case of PEDOT:PSS occurs via cation migration, while for the others it is mainly anion migration. This inhibition is particularly long lasting when the PEDOT:PSS is applied on an iron substrate, whereas on zinc the high potential is maintained for a period circa ten times shorter.

One aim should be to increase the percentage of the formed protection zones at the interface, which will lead to a significant increase of the resistance to cathodic delamination.

In the moment an empirical approach for optimizing the size and amount of ICP particles for providing optimal performance by experiments is still necessary. To obtain a better understanding about mobility at the buried interface, which determines the interfacial re-

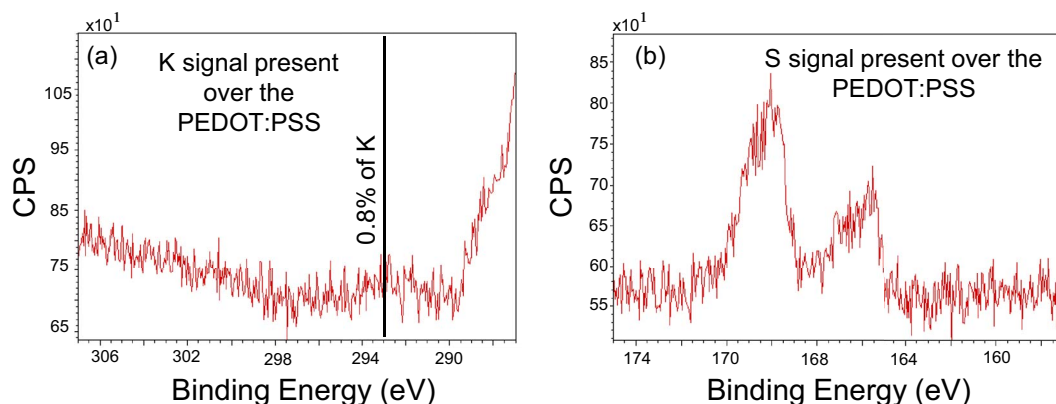


Figure 8. XPS spectra of potassium (a) and sulfur (b) on top of the PEDOT:PSS dot, for sample (II). From (a) it can be deduced that the PEDOT:PSS incorporates potassium cations migrating from the defect, while (b) shows the typical S2p peaks at ~ 168 and ~ 164 eV, indicating (together with their absence in regions A-C) that the PSS anions are trapped inside the ICP.

sistance, is object of current research and may hopefully provide tools for a more knowledge based design.

Acknowledgments

A. Merz acknowledges the Max-Planck Society for funding. M. Rohwerder gratefully acknowledges the financial support from DFG SPP 1568 “Design and Generic Principles of Self-Healing Materials”.

ORCID

A. Merz  <https://orcid.org/0000-0003-2403-7177>

M. Rohwerder  <https://orcid.org/0000-0002-2466-3963>

References

1. S. Sindhu, K. N. Rao, S. Ahuja, A. Kumar, and E. S. R. Gopal, *Mat Sci Eng B-Solid*, **132**(1-2), 39 (2006).
2. K. H. Yeoh, N. A. Talik, T. J. Whitcher, C. Y. B. Ng, and K. L. Woon, *J Phys D Appl Phys*, **47**(20), (2014).
3. K. Sun, S. P. Zhang, P. C. Li, Y. J. Xia, X. Zhang, D. H. Du, F. H. Isikgor, and J. Y. Ouyang, *J Mater Sci-Mater El*, **26**(7), 4438 (2015).
4. C. F. Glover, J. McGettrick, G. Williams, T. M. Watson, and D. Bryant, *J Electrochem Soc*, **162**(10), H799 (2015).
5. Y. W. Shao, C. Jia, G. Z. Meng, T. Zhang, and F. H. Wang, *Corros Sci*, **51**(2), 371 (2009).
6. A. J. Heeger, *Rev Mod Phys*, **73**(3), 681 (2001).
7. A. G. MacDiarmid, *Rev Mod Phys*, **73**(3), 701 (2001).
8. H. Shirakawa, *Rev Mod Phys*, **73**(3), 713 (2001).
9. M. Rohwerder and A. Michalik, *Electrochim Acta*, **53**(3), 1300 (2007).
10. A. Michalik and M. Rohwerder, *Z Phys Chem*, **219**(11), 1547 (2005).
11. M. Rohwerder, *Int J Mater Res*, **100**(10), 1331 (2009).
12. A. Merz, M. Uebel, and M. Rohwerder, *J Electrochem Soc*, **166**, 304 (2019).
13. D. Vijayshankar, A. Altin, C. Merola, A. Bashir, E. Heinen, and M. Rohwerder, *J Electrochem Soc*, **163**(13), C778 (2016).
14. A. Leng, H. Streckel, and M. Stratmann, *Corros Sci*, **41**(3), 547 (1999).
15. A. Vimalanandan, *Ruhr-Universität Bochum*, 2016.
16. M. Rohwerder, S. Isik-Uppenkamp, and C. A. Amarnath, *Electrochim Acta*, **56**(4), 1889 (2011).
17. M. Rohwerder, L. Duc, and A. Michalik, *Electrochim Acta*, **54**(25), 6075 (2009).
18. G. Williams and H. N. McMurray, *Electrochim Solid St*, **8**(9), B42 (2005).
19. V. Shkirskiy, M. Uebel, A. Maltseva, G. Lefèvre, P. Volovitch, and M. Rohwerder, *npj Materials Degradation*, **3**(1), 2 (2019).